The Effect of Timing Offset on Fractionally-Spaced CMA

P. Schniter and C.R. Johnson, Jr.

March 16, 1998

1 Introduction

In this paper, we analyze the impact that choice sampling phase has on the transient and steady-state behaviors of FSE-CMA. Our analysis is enabled by the introduction of an *interpolation operator* into the standard FSE system model.

2 System Model

Consider the $T/2$-spaced equalization scenario illustrated by Figure 2. A T-spaced source process $\{s_n\}$ is transmitted through a baseband-equivalent channel with impulse response $h(t)$ and bandlimited[1] additive noise process $w(t)$. The received signal $x(t)$ is sampled (uniformly) at $T/2$-spaced intervals, and the resulting sequence $r_k = x\big((k-\rho)T/2\big)$ is applied to an FIR equalizer with length-N_f impulse response vector $\mathbf{f}$. The delay parameter $\rho \in (-1, 1)$ allows for an arbitrary sampling phase offset. Finally, the equalizer output is decimated in forming the soft decisions $\{y_n\}$.

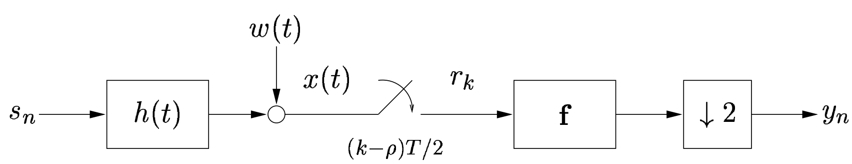

Figure 1: $T/2$-spaced equalization model, showing channel $h(t)$, additive noise $w(t)$, sampling phase offset ρ, and fractionally-spaced equalizer $\mathbf{f}$.

The discrete multirate equivalent of Figure 1 is shown in Figure 2, where the continuous-time channel response, noise, and channel output have been replaced by their $T/2$-sampled equivalents: $h_k = h(kT/2)$, $w_k = w(kT/2)$, and $x_k = x(kT/2)$. Assuming an FIR channel, the nonzero channel samples can be collected into a length-N_h impulse response vector $\mathbf{c}$. In the discrete model, the receiver sampling phase offset is implemented by the interpolation operator $\mathbf{T}_\rho$, effecting the equivalent of a $\rho T/2$ second delay from $\{x_k\}$ to $\{r_k\}$. The construction of $\mathbf{T}_\rho$ will be discussed in Section 3.

The baud-spaced system response taking $\{s_n\} \to \{y_n\}$ is characterized by the length-N_q vector $\mathbf{q}$, so that in the absence of noise $y_n = \mathbf{s}^t(n)\mathbf{q}$, where $\mathbf{s}(n) = (s_n, s_{n-1}, \dots, s_{n-N_q+1})^t$ is a

[1]For simplicity, we assume that $w(t)$ is bandlimited to $|\omega| < 2\pi/T$.

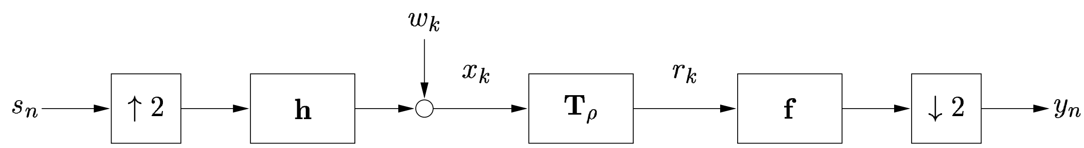

Figure 2: Discrete system model, with interpolation operator $\mathbf{T}_\rho$ implementing $\rho T/2$-second sampling phase offset.

vector of previous source symbols at time n. The $N_q \times N_f$ channel matrix

$$\mathbf{H} = \begin{pmatrix} h_1 & h_0 & & & & & \\ h_3 & h_2 & h_1 & h_0 & & & \\ \vdots & \vdots & h_3 & h_2 & \ddots & h_1 & h_0 \\ h_{N_h-1} & h_{N_h-2} & \vdots & \vdots & & h_3 & h_2 \\ & & h_{N_h-1} & h_{N_h-2} & \ddots & \vdots & \vdots \\ & & & & & h_{N_h-1} & h_{N_h-2} \end{pmatrix}$$

is constructed so that $\mathbf{q} = \mathbf{Hf}$ (in the case of zero sampling phase offset, i.e., $\rho = 0$) [1]. Collecting the previous N_f channel output and noise samples into $\mathbf{x}(n)$ and $\mathbf{w}(n)$, respectively, yields $\mathbf{x}(n) = \mathbf{H}^t\mathbf{s}(n) + \mathbf{w}(n)$. The timing phase offset between $\mathbf{x}(n)$ and $\mathbf{r}(n)$ may be approximated by an interpolation operator $\mathbf{T}_\rho \in \mathbb{R}^{N_f \times N_f}$:

$$\mathbf{r}(n) = \mathbf{T}_\rho \mathbf{x}(n). \tag{1}$$

In this case, the system response incorporating $\rho T/2$ seconds of sampling offset takes the form

$$\mathbf{q} = \mathbf{H}\mathbf{T}_\rho^t \mathbf{f}. \tag{2}$$

Section 4 discusses how this $\mathbb{R}^{N_f \times N_f}$ construction of $\mathbf{T}_\rho$ is a particular case of a more general (and arbitrarily accurate) construction.

3 The Interpolation Operator

The following sections detail the construction of interpolation operators acting on finite-length sampled data records which approximate the action of the continuous-time delay operator

$$\mathbf{T}_\rho^{(c)} : x(t) \mapsto x(t - \rho T/2) = \int_{-\infty}^{\infty} x(\tau)\delta(t - \rho T/2 - \tau)d\tau, \tag{3}$$

where $\delta(t)$ denotes the Dirac delta.

3.1 Construction of $\mathbf{T}_\rho$

Fourier theory specifies that the frequency domain equivalent of (3) is

$$\hat{\mathbf{T}}_\rho^{(c)} : X(e^{j\omega}) \mapsto e^{-j\omega\rho T/2} X(e^{j\omega}), \tag{4}$$

where $X(e^{j\omega})$ is the Fourier transform of $x(t)$.

The frequency domain definition (4) motivates our treatment of discrete-time signals. First, however, we establish some common notation. Let $\mathbf{x} \in \mathbb{C}^N$ denote a vector of time-domain samples and $\hat{\mathbf{x}} \in \mathbb{C}^N$ denote its DFT, such that

$$\hat{x}_m = \frac{1}{\sqrt{N}} \sum_{k=0}^{N-1} x_k e^{-j2\pi mk/N} \quad \text{for} \quad 0 \leq m \leq N-1.$$

The DFT has an equivalent matrix representation $\mathbf{W} \in \mathbb{C}^{N \times N}$ where

$$[\mathbf{W}]_{m,n} = \frac{1}{\sqrt{N}} e^{-j2\pi mn/N},$$

so that $\hat{\mathbf{x}} = \mathbf{W}\mathbf{x}$. It is important to note that $\mathbf{W}$ is both unitary ($\mathbf{W}\mathbf{W}^H = \mathbf{W}^H\mathbf{W} = \mathbf{I}$) and symmetric ($\mathbf{W} = \mathbf{W}^t$). For notational simplicity, we henceforth assume that N is even.

Consider the discrete equivalent of the frequency domain operator in (4):

$$\hat{\mathbf{T}}_\rho : \hat{\mathbf{x}} \mapsto \mathbf{\Phi}\hat{\mathbf{x}},$$

where $\mathbf{\Phi}$ is a diagonal matrix with entries

$$[\mathbf{\Phi}]_{m,m} := \begin{cases} e^{-j2\pi\rho m/N} & 0 \leq m < N/2, \\ 1 & m = N/2, \\ e^{-j2\pi\rho(m-N)/N} & N/2 < m \leq N-1. \end{cases} \tag{5}$$

The conjugate symmetry along the diagonal of $\mathbf{\Phi}$ ensures that the corresponding time-domain operation

$$\mathbf{T}_\rho : \mathbf{x} \mapsto \mathbf{W}^H \mathbf{\Phi} \mathbf{W} \mathbf{x} \tag{6}$$

is real-valued. The properties listed below follow from inspection:

Claim 1. *The operator $\mathbf{T}_\rho \in \mathbb{R}^{N \times N}$ defined in (6) has the following properties:*

1. *$\mathbf{T}_\rho$ is unitary,*
2. *$\mathbf{T}_\rho = \mathbf{T}^t_{-\rho}$,*
3. *$\mathbf{T}_\rho$ is circulant.*

Figure 3 demonstrates the interpolation capabilities of $\mathbf{T}_\rho$ using SPIB[2] channel #1 and various values of ρ.

4 Application of $\mathbf{T}_\rho$

The frequency-domain construction (6) implies that $\mathbf{T}_\rho$ implements a "circulant" resampling; i.e., $\{x_k\}$ are treated as samples of a cyclic waveform $x(t)$ on $(-\infty, \infty)$ with the property that $x(t) = x(t - NT/2)\ \forall t$ where $x_k = x(kT/2)$.

[2] The Rice University Signal Processing Information Base (SPIB) microwave channel database resides at `http://spib.rice.edu/spib/microwave.html`.

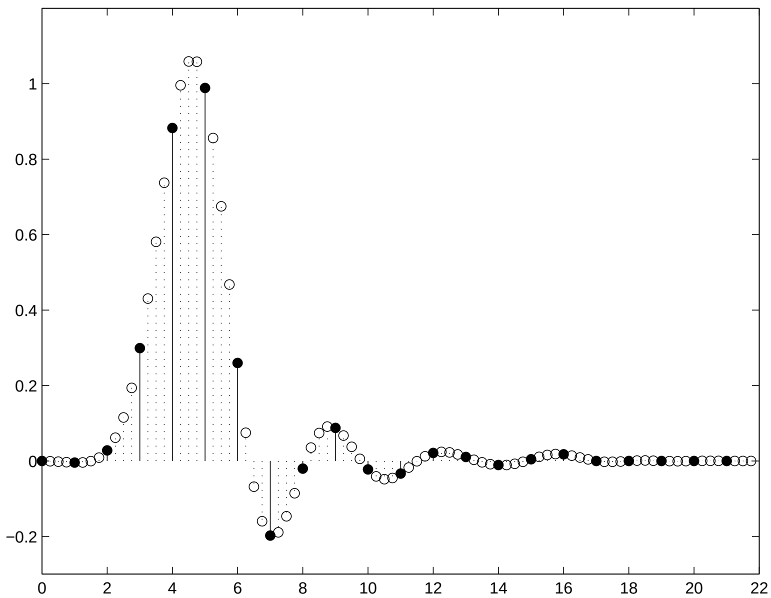

Figure 3: SPIB impulse response interpolated using four values of ρ. Solid stems indicate the original $T/2$-spaced samples, while dotted stems indicate the delayed versions obtained using $\mathbf{T}_\rho$ with $\rho = \{0, 0.25, 0.5, 0.75\}$.

Though I have not proved it yet, I believe that $\mathbf{T}_\rho$ in (6) is the best L_2 approximation of (3) over $\mathbb{R}^{N \times N}$. Note, however, that a frequency-weighted L_2 design may better suit the signals typically encountered in the $T/2$-spaced equalization scenario. Does such a $\mathbf{T}_\rho$ still satisfy the properties in Claim 1? What about the following H_∞-like optimization?

$$\begin{aligned} \mathbf{T}_\rho &:= \arg \min_{\mathbf{T} \in \mathbb{R}^{N \times N}} \max_{\mathbf{x} \in \mathbb{R}^N} \frac{\| \sum_n [\mathbf{T}\mathbf{x}]_n e^{-j\omega n} - D_\rho(\omega) \sum_n [\mathbf{x}]_n e^{-j\omega n} \|_{L_2}}{\|\mathbf{x}\|_2}, \quad \text{where} \\ D_\rho(\omega) &:= e^{-j\omega\rho} \text{ for } \omega \in (-\pi, \pi). \end{aligned}$$

5 Applications of the Delay Operator

As suggested earlier, the delay operator in (6) may prove useful in FSE analysis. Consider the SVD of the (non-delayed) real-valued channel convolution matrix: $\mathbf{H} = \mathbf{U}\mathbf{S}\mathbf{V}^t$. Incoporating the delay operator into the convolution operation yields the matrix

$$\bar{\mathbf{H}} := \mathbf{H}\mathbf{T}_\rho^t = \mathbf{U}\mathbf{S}\mathbf{V}^t\mathbf{T}_\rho^t = \mathbf{U}\mathbf{S}(\mathbf{T}_\rho\mathbf{V})^t = \mathbf{U}\mathbf{S}\bar{\mathbf{V}}^t, \tag{7}$$

where the unitary property of $\mathbf{T}_\rho$ implies that $\bar{\mathbf{V}} := \mathbf{T}_\rho\mathbf{V}$ is also unitary. In other words, the ρ-delay leads to a convolution-matrix-like quantity $\bar{\mathbf{H}}$ with SVD $\bar{\mathbf{H}} = \mathbf{U}\mathbf{S}\bar{\mathbf{V}}^t$ and preserves the singular values and left singular vectors of $\mathbf{H}$. As it is known that $\mathbf{V}$ determines the orientation of CMA regions of convergence in equalizer space [Chung:Draft:ROC], the unitary transformation $\mathbf{T}_\rho$ describes the rotation of ROC boundaries as a function of sampling phase.

Now consider noise entering the system of Figure 2 just after the channel. The combined operation of delay plus equalization can be represented by the modified equalizer impulse response vector

$$\bar{\mathbf{f}} := \mathbf{T}_\rho^t \mathbf{f}. \tag{8}$$

The CMA cost function, for source and noise processes both white and real-valued, then takes the form

$$J_{CM}|_{\mathbb{R}} \;=\; (\kappa_s - 3)\sum_{i=0}^{P-1} h_i^4 + 3\|\mathbf{q}\|_2^4 + 3\sigma_w^4\|\bar{\mathbf{f}}\|_2^4 + 6\sigma_w^2\|\mathbf{q}\|_2^2\|\bar{\mathbf{f}}\|_2^2 - 2\kappa_s\big(\|\mathbf{q}\|_2^2 + \sigma_w^2\|\bar{\mathbf{f}}\|_2^2\big) + \kappa_s^2$$

where σ_w^2 is the noise variance and κ_s is the (normalized) source kurtosis. But since the unitary operation $\mathbf{T}_\rho$ preserves both the ℓ_2 norm and the reachable system subspace (as confirmed by SVD above), the CMA cost function remains essentially invariant to changes in sampling time offset. This contradicts the (unconvincing) claims of [2]. Simulations should be performed as a confirmation.

6 Other Questions

- Relationships to Zak Transform [3]?

References

[1] C.R. Johnson, Jr., P. Schniter, et al., "Blind equalization using the constant modulus criterion: A review," Proceedings of the IEEE, *Special Issue on Blind System Identification and Equalization*, Sep. 1998.

[2] J.K. Tugnait, "On fractionally spaced blind adaptive equalization under symbol timing offsets using Godard and related equalizers," IEEE Transactions on Signal Processing, vol. 44, no. 7, pp. 1817-21, July 1996.

[3] J.W.M. Bergmans and A.J.E.M. Janssen, "Robust data equalization, fractional tap spacing and the Zak transform," Philips Journal of Research, vol. 42, no. 4, pp. 351-398, 1987.